DOI: 10.1002/ejic.201100625

Oxidovanadium(IV) Complexes of Tetradentate Ligands Encapsulated in Zeolite-Y as Catalysts for the Oxidation of Styrene, Cyclohexene and Methyl Phenyl Sulfide

Mannar R. Maurya,*[a] Priyanka Saini,[a] Amit Kumar,[b] and João Costa Pessoa*[b]

Keywords: Heterogeneous catalysis / Vanadium / Oxidation / EPR spectroscopy

The reaction of oxidovanadium(IV)-exchanged zeolite-Y with *N*,*N*′-ethylenebis(pyridoxyliminato) (H_2pydx-en, **I**), *N*,*N*′-propylenebis(pyridoxyliminato) (H_2pydx-1,3-pn, **II**) and H_2pydx-1,2-pn (**III**) in methanol heated at reflux leads to the formation of the corresponding complexes, abbreviated herein as [V^{IV}O(pydx-en)]-Y (**4**), [V^{IV}O(pydx-1,3-pn)]-Y (**5**) and [V^{IV}O(pydx-1,2-pn)]-Y (**6**) in the supercages of zeolite-Y. The neat complexes [V^{IV}O(pydx-en)] (**1**), [V^{IV}O(pydx-1,3-pn)] (**2**) and [V^{IV}O(pydx-1,2-pn)] (**3**) were also prepared. Spectroscopic studies (IR, UV/Vis and EPR), elemental analyses, thermal studies, field-emission scanning electron micrographs (FESEM) and X-ray diffraction patterns were used to characterize these complexes. Oxidations of styrene, cyclohexene and methyl phenyl sulfide were investigated using these complexes as catalyst precursors in the presence of H_2O_2 as oxidant. Under the optimized reaction conditions, a maximum of 85.5 % conversion of styrene was obtained with **4**, 84.6 % conversion with **5** and 82.9 % conversion with **6** in 6 h of reaction time. The selectivity of the various products was similar for the catalyst precursors **4**–**6** and followed the order: benzaldehyde > 1-phenylethane-1,2-diol > benzoic acid > phenyl acetaldehyde. With cyclohexene, a maximum conversion of 95.9 % was achieved with **4**, 94.5 % with **5** and 94.2 % conversion with **6**, also in 6 h of reaction time. The selectivity of the various products was similar for the three catalysts: 2-cyclohexen-1-one > 2-cyclohexen-1-ol > cyclohexane-1,2-diol. The oxidation of methyl phenyl sulfide was achieved with **4**, **5** and **6** in 2.5 h of reaction time with 85.5, 82.1 and 80 % conversion, with higher selectivity towards sulfoxide. Overall, the encapsulated catalysts were significantly more active than their neat counterparts and have the further advantage of being recyclable. No relevant difference in activity was found due to a change in the diamine in the Schiff base ligands **I**–**III**. UV/Vis and ^{51}V NMR spectroscopic experiments with **1** confirmed the plausible formation of $V^{V}O(O_2)$**L** as intermediates in the catalytic oxidations.

Introduction

The advantages of zeolite-encapsulated metal complexes (ZEMC) as catalysts in the past two decades have promoted researchers to design such catalysts and investigate their catalytic properties.[1–7] The relatively large size of the encapsulated catalysts and their rigidity make it difficult for them to escape from the zeolite cages. Thus, zeolite-encapsulated homogeneous catalysts may have the advantages of solid heterogeneous catalysts while retaining most of their original character. The relatively easy preparation, wide variety and flexible nature of salen-type [salen = *N*,*N*′-ethylenebis(salicylimine)] ligands have provided opportunities to encapsulate various transition-metal complexes in the nanocavity of zeolites and to develop catalytic processes for various reactions. Poltowicz et al. encapsulated a whole range of salen complexes {e.g., [Fe(salen)], [Mn(salen)], [Cu(salen)] and [Co(salen)]} in zeolite-X and studied their catalytic activity for the oxidation of cyclooctane.[8] Ratnasamy and co-workers used copper(II) and manganese(III) complexes of salen derivatives encapsulated in the cavity of zeolite-X and zeolite-Y for the oxidation of styrene under aerobic conditions using *tert*-butyl hydroperoxide as oxidant. The catalytic efficiency of these encapsulated complexes was much higher than that of the neat complexes. Electron-withdrawing substituents such as Cl, Br and NO_2 on the aromatic ring were found to enhance the rate of oxidation.[9,10] These complexes also catalyze the oxidation of phenol and *p*-xylene.[11,12] Epoxidations of cyclohexene, cyclooctene, 1-hexene and other various types of alkenes, arenes and cycloalkenes, catalyzed by different complexes of salen-type ligands, were also carried out.[2,13–15] [Co(salophen)]-Y [H_2salophen = *N*,*N*′-bis(salicylidene)benzene-1,2-diamine] and related derivatives catalyzed the oxi-

[a] Department of Chemistry,
Indian Institute of Technology Roorkee,
Roorkee 247667, India
Fax: +91-1332-273560
E-mail: rkmanfcy@iitr.ernet.in
[b] Centro Química Estrutural, Instituto Superior Técnico,
Technical University of Lisbon,
Av. Rovisco Pais, 1049-001 Lisboa, Portugal
Fax: +351-21-8464455
E-mail: joao.pessoa@ist.utl.pt
Supporting information for this article is available on the WWW under http://dx.doi.org/10.1002/ejic.201100625.

dation of β-isophorone (βIP) to ketoisophorone (KIP) under ambient conditions of temperature and pressure.[16] Liquid-phase oxidation of phenol with H_2O_2 was reported using Cu^{II} and $V^{IV}O$ complexes of *N*,*N*′-bis(salicylidene)-propane-1,3-diamine (H_2sal-1,3-pn) and *N*,*N*′-bis(salicylidene)diethylenetriamine (H_2saldien).[17–19] Zeolite-Y-encapsulated Cu^{II} and $V^{IV}O$ complexes of *N*,*N*′-bis(salicylidene)-cyclohexane-1,2-diamine (H_2sal-dach) catalyze the oxidation of styrene, cyclohexene and cyclohexane efficiently.[20] Similar homogeneous oxidovanadium(IV) complexes derived from 2,2′-dimethylpropanediamine catalyze the oxidation, by *tert*-butyl hydroperoxide, of cyclooctene and styrene.[21] Chiral [Mn^{III}(salen)]-type complexes immobilized on inorganic–organic hybrid materials of zirconium poly(styrene-phenylvinylphosphonate)phosphate were also used as effective catalysts for asymmetric epoxidation of unfunctionalized olefins.[22,23]

We reported several chiral V-salen and V-salan (H_2salan = reduced Schiff bases) complexes and tested them as catalysts in the oxidation of styrene, cyclohexene, cumene and methyl phenyl sulfide using H_2O_2 and *t*BuOOH as oxidants. Overall, the V-salan complexes showed higher activity and normally better selectivity in alkene oxidation and higher activity and enantioselectivity for sulfoxidation than their parent V-salen complexes.[24] The catalytic potential, often with high turnover numbers, of metal complexes encapsulated in the nanocavity of zeolites prompted us to design new zeolite-Y-encapsulated oxidovanadium(IV) complexes of tetradentate ligands **I**, **II** and **III** (Scheme 1). We have also prepared the corresponding neat oxidovanadium(IV) complexes of these ligands to compare their catalytic potentials.

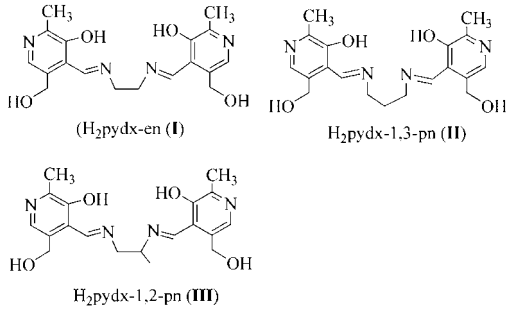

Scheme 1. Structural formulas of ligands and abbreviations used in this work.

Several authors state[25] that the flexibility of the diamine backbone of the Schiff base ligand and the stereoelectronic effects of substituents are crucial factors that govern the reactivity of complexes. To test the influence of change in the diamine moiety and to further understand how this factor is affected by encapsulation of the complexes in the cavities of zeolite-Y, three heterogenized complexes **4**–**6** were prepared.

Ligands **I**–**III** include the $N_{pyridine}$ atom and the –CH_2OH group of the pyridoxal moiety. This anticipates the probable formation of hydrogen bonds of these groups with surface –OH groups inside the cavities of zeolite-Y. Besides restricting the movement of complexes inside the zeolite cages, this may (or may not) induce selectivity effects distinct from those of the corresponding Schiff base complexes derived from the condensation of salicylaldehyde with diamine derivatives.

It is expected that the access of the oxidant and substrate to the active complex inside the zeolite cages is rather restricted, and further knowledge how this may affect the overall efficiency of the reactions is required. Moreover, the inside of the zeolite cages has polarity and hydrogen-bond formation capability quite distinct from organic solvents such as acetonitrile, and it is relevant to check if, when using aqueous H_2O_2 as oxidant, this may favour the activity when comparing encapsulated and nonencapsulated catalysts.

Results and Discussion

Synthesis and Characterization of Complexes

The reaction between equimolar amounts of [V^{IV}O(acac)$_2$] and H_2pydx-en (**I**), H_2pydx-1,3-pn (**II**), or H_2pydx-1,2-pn (**III**) (Scheme 1) in dry methanol heated at reflux yielded the $V^{IV}O$ complexes [V^{IV}O(pydx-en)] (**1**), [V^{IV}O(pydx-1,3-pn)] (**2**) and [V^{IV}O(pydx-1,2-pn)] (**3**), respectively. The general synthetic process may be outlined by Equation (1).

$$[V^{IV}O(acac)_2] + \mathbf{L}H_2 \rightarrow [V^{IV}OL] + 2Hacac \quad (1)$$

$H_2\mathbf{L}$ = H_2pydx-en: **1**; $H_2\mathbf{L}$ = H_2pydx-1,3-pn: **2**; $H_2\mathbf{L}$ = H_2pydx-1,2-pn: **3**.

Scheme 2 presents the structural formulas and binding sets proposed for these complexes, and are based on their spectroscopic characterization [IR, electronic, electron paramagnetic resonance (EPR)] and elemental analyses. The coordination of the ligands involves their dianionic ($ONNO^{2-}$) form.

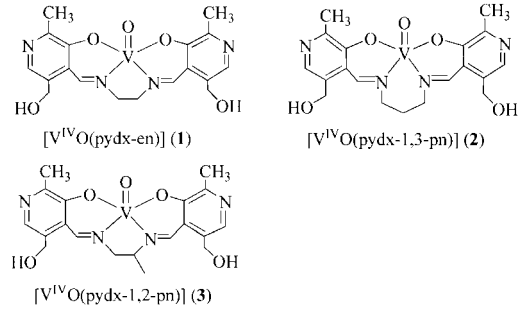

Scheme 2. Structural formulas of the neat complexes prepared in this work.

Encapsulation of [V^{IV}O(pydx-en)] (**1**), [V^{IV}O(pydx-1,3-pn)] (**2**) and [V^{IV}O(pydx-1,2-pn)] (**3**) in the nanocavities of zeolite-Y involved as a first step the exchange of $[V^{IV}O]^{2+}$ with Na^+ of Na–Y in water to form zeolite-[V^{IV}O]-Y species. This is followed by the reaction of the metal-exchanged zeolite-Y with **I**, **II** or **III** in methanol to give [V^{IV}O(pydx-en)]-Y (**4**), [V^{IV}O(pydx-1,3-pn)]-Y (**5**) and [V^{IV}O(pydx-1,2-

pn)]-Y (**6**). The remaining uncomplexed metal ions in zeolite were removed by ion exchange with aqueous 0.01 M NaCl solution. Extraction of impurities with methanol was carried out by Soxhlet extraction, thus removing the excess amount of free ligand. As the solids were submitted to very extensive extraction, we expect that the metal content found (Table 1) after encapsulation is only due to the presence of $V^{IV}O$ complexes inside the cavities of the zeolite-Y. The diagonal dimension of the closely related complex, [Cu^{II}-(pydx-en)][26] is around 12 Å, which suggests that they will fit well into the super cages of the zeolite-Y and will not pass through the apertures of around 7.4 Å.[27]

Table 1. Chemical composition, physical and analytical data.

	Colour	Metal content [wt.-%]	Metal content [mmol g^{-1}]
[VO(pydx-en)]-Y (**4**)	light green	1.78	0.35
[VO(pydx-1,3-pn)]-Y (**5**)	light green	1.85	0.36
[VO(pydx-1,2-pn)]-Y (**6**)	light cream	1.53	0.29

These encapsulated complexes were additionally characterized by thermogravimetric patterns, field-emission scanning electron micrograph (FESEM), energy-dispersive X-ray analysis (EDX), powder X-ray diffraction (PXRD) studies and EPR. The binding modes for these encapsulated complexes are proposed by comparison with the corresponding homogeneous model complexes.

Thermogravimetric Analysis

The thermal decomposition of [$V^{IV}O$(pydx-1,3-pn)]-Y (**5**) and [$V^{IV}O$(pydx-1,2-pn)]-Y (**6**) proceeds in two major steps. An endothermic weight loss of around 21% in **5** and around 20% in **6** occurs in the temperature range 100 to 300 °C, which is possibly due to the removal of intrazeolitic water. The second step of endothermic weight loss starts immediately after the first one and continues till around 600 °C to constant weight. A total weight loss of approximately 6% in **5** and 7% in **6** occurs in the temperature range of 300–600 °C due to the slow decomposition of vanadium complexes. The first decomposition step of complex [VO(pydx-en)]-Y (**4**) is similar but continues to around 350 °C with a weight loss of 25%. The second step of endothermic weight loss of approximately 16% starts immediately after the first step and consists of several substeps that continue till around 650 °C to constant weight. This information suggests the insertion of only a small amount of metal complexes in the cavities of the zeolite-Y. This is in agreement with the low percentage of metal content obtained for encapsulated complexes (Table 1).

PXRD Studies

The PXRD patterns of Na–Y, [$V^{IV}O$]–Y and encapsulated $V^{IV}O$ complexes were recorded at 2θ values between 5 and 70°. The PXRD patterns of representative $V^{IV}O^{2+}$-exchanged zeolite and the zeolite-encapsulated metal complexes along with Na–Y are presented in Figure 1. The diffraction pattern of encapsulated metal complexes, [$V^{IV}O$]–Y and Na–Y are essentially similar except for a slight change in the intensity of the bands in encapsulated complexes. These observations indicate that the framework of zeolite did not undergo any significant structural change during encapsulation (i.e., the crystallinity of the zeolite-Y is preserved). Absence or no formation of new peaks due to the presence of complexes was detected in encapsulated zeolites.

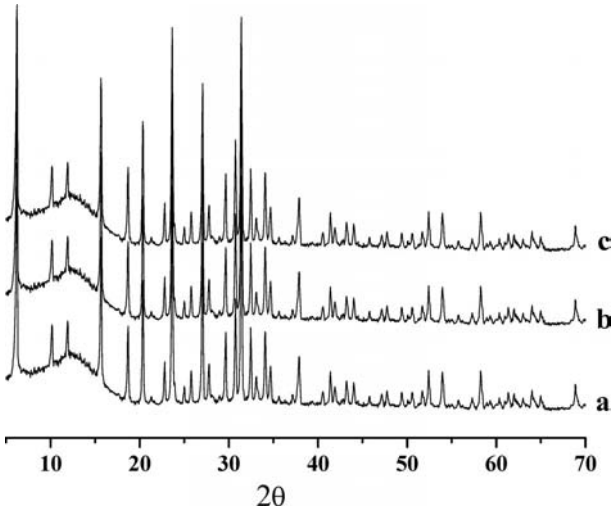

Figure 1. PXRD patterns of (a) Na–Y, (b) [$V^{IV}O$]-Y and (c) [$V^{IV}O$-(pydx-en)]-Y (**4**).

FESEM and EDX Study

Figure 2 presents the field-emission scanning electron micrograph of [$V^{IV}O$(pydx-en)]-Y (**4**). It is clear from the micrograph that zeolite-entrapped vanadium complexes have well-defined crystals, and there is no indication of the presence of any metal ions or complexes on the surface. EDX plots support this conclusion as no vanadium or nitrogen contents were noted on the spotted surfaces in plots. The average silicon and aluminium percentage on the spotted surface, as evaluated semiquantitatively, were approximately 7.5 and 2.6%, respectively. The finding of around 1.1% sodium suggests the exchange of surface free $V^{IV}O^{2+}$ ions by sodium ions during the re-exchange process (see Exp. Sect.). Only a small amount of carbon (about 18.4%) but no nitrogen suggests the presence of a trace amount of solvent (methanol) from which it was finally washed after Soxhlet extraction. No morphological changes on the surface upon encapsulation of the complexes in the cavities were noticed. Very similar observations were obtained for the other two catalysts.

IR Spectral Studies

A partial list of IR spectroscopic data is presented in Table 2. Comparison of the spectra of neat complexes with the respective ligand provides evidence for the coordinating mode of ligands in complexes. Globally the intensities of

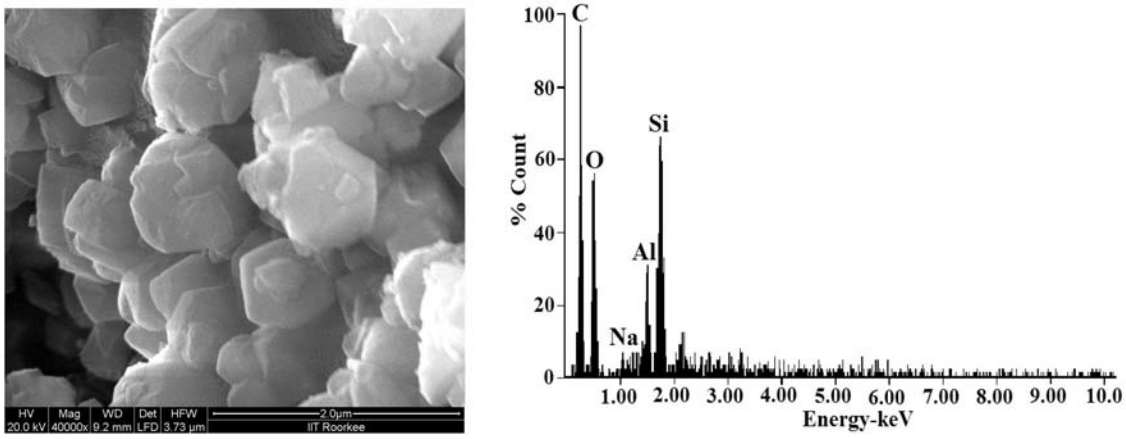

Figure 2. Field-emission scanning electron micrograph of [V^{IV}O(pydx-en)]-Y and the corresponding energy-dispersive X-ray analysis plot.

the peaks due to encapsulated complexes are weak because of their low amount in zeolite matrix and the spectra of the encapsulated as well as neat complexes showed essentially similar bands. Ligands as well as complexes exhibit several multiple bands of medium intensity that cover the region 2850–3000 cm^{-1} due to C–H bands. A medium-intensity band around 3000 cm^{-1} in ligands, mostly due to intramolecular $\nu(OH)_{phenolic}$ hydrogen bonding, was not found in the spectra of encapsulated as well as neat complexes, thus indicating the destruction of the hydrogen-bond network followed by the coordination of the phenol oxygen atom after deprotonation. A sharp band that appeared at 1630 cm^{-1} (in **I**), at 1634 cm^{-1} (in **II**) and at 1631 cm^{-1} (in **III**), due to the ν(C=N) (azomethine) shifts in complexes, thereby suggesting the coordination of the azomethine nitrogen atom. All neat $V^{IV}O$ complexes show a sharp band between 973–986 cm^{-1} due to ν(V=O).[28] This band was not observed in encapsulated complexes, probably due to poor loading of complexes in the zeolite matrix.

Table 2. IR spectroscopic data of ligand, neat and encapsulated complexes.

	ν(C=N) [cm^{-1}]	ν(V=O) [cm^{-1}]
H_2pydx-en (**I**)	1630	–
H_2pydx-1,3-pn (**II**)	1634	–
H_2pydx-1,2-pn (**III**)	1631	–
[V^{IV}O(pydx-en)] (**1**)	1618	984
[V^{IV}O(pydx-1,3-pn)] (**2**)	1625	983
[V^{IV}O(pydx-1,2-pn)] (**3**)	1627	973
[V^{IV}O(pydx-en)]-Y (**4**)	1619	–
[V^{IV}O(pydx-1,3-pn)]-Y (**5**)	1633	–
[V^{IV}O(pydx-1,2-pn)]-Y (**6**)	1630	–

Electronic Spectral Studies

The electronic spectroscopic data of ligands and complexes are presented in Table 3. The spectral profiles of neat complexes are reproduced in Figure S1 (see the Supporting Information), where those of encapsulated ones are in Figure 3. The electronic absorption spectra of [V^{IV}O(pydx-en)] was described previously.[29] The broad band of medium intensity at around 380 nm in neat complexes is due to both (i) the ligand-to-metal charge-transfer (phenolate O to d orbitals of vanadium) band, and (ii) the n→π* transition of the C=N moiety. The bands at around 275 nm and around 235 nm may be assigned to π→π* and ϕ→ϕ* transitions,

Table 3. Electronic spectroscopic data of ligands: neat and in complexes.

	Solvent	λ[a] [nm]
H_2pydx-en (**I**)	MeOH	336, 254, 215
H_2pydx-1,3-pn (**II**)	MeOH	418, 335, 253, 214
H_2pydx-1,2-pn (**III**)	MeOH	336, 253, 211
[V^{IV}O(pydx-en)] (**1**)	MeOH	766, 591, 380, 263b, 234
	DMSO	750b, 585, 385, 281b, 262
[V^{IV}O(pydx-1,2-pn)] (**3**)	MeOH	787, 594, 383, 312b, 274b, 239
	DMSO	750b, 590, 385, 280b, 262
[V^{IV}O(pydx-1,3-pn)] (**2**)	MeOH	383, 311b, 274b, 239
	DMSO	774, 538
[V^{IV}O(pydx-en)]-Y (**4**)	nujol	393, 344, 295, 221
[V^{IV}O(pydx-1,3-pn)]-Y (**5**)	nujol	415, 340, 273, 228
[V^{IV}O(pydx-1,2-pn)]-Y (**6**)	nujol	415, 288, 223

[a] b indicates broad band.

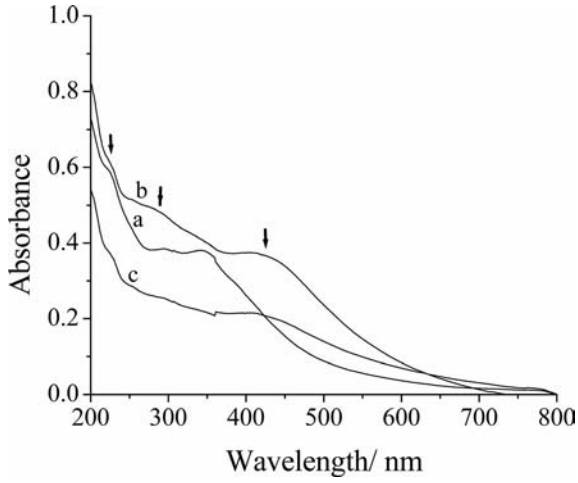

Figure 3. Electronic spectra of (a) [V^{IV}O(pydx-en)]-Y (**4**), (b) [V^{IV}O(pydx-1,3-pn)]-Y (**5**) and (c) [V^{IV}O(pydx-1,2-pn)]-Y (**6**) recorded dispersed in Nujol.

respectively. These are sometimes designated by B band and K band, respectively.[30] In addition, two broad bands at around 750 and 580 nm (in DMSO) appear in the visible region and are assigned to band I ($d_{xy} \rightarrow d_{xz}$, d_{yz}) and band II ($d_{xy} \rightarrow d_{x^2-y^2}$). All these bands show slight shifts in methanol.[31]

Due to poor loading of complexes in the nanocavities of zeolite-Y, and their intrinsic low intensity, the bands due to d–d transitions are not observed in **4**–**6**. However, all encapsulated complexes exhibit three bands in the UV region and the band at around 400 nm, thereby suggesting the presence of the $V^{IV}O$ complexes in the cavities of zeolite-Y.

EPR Studies

The EPR spectra of "frozen" (77 K) solutions of **1**, **2** and **3** in MeOH or DMSO are depicted in Figure 4, and those of solids **4**, **5** and **6** at room temperature in Figure 5. The spectra of **1**–**3** are well resolved, whereas the spectra of **4**–**6** show broadening and changes in the peak-to-peak line widths due to incomplete rotational averaging of the *g* and *A* tensors.[32] These broadened spectra, when compared with those of other V^{IV}-heterogenized complexes[1] indicate that the encapsulated V^{IV} complexes closely fit the zeolite cages; additionally, the compounds probably have their movement restricted by hydrogen-bond formation between OH groups of zeolite and $N_{pyridine}$ and/or $-CH_2OH$ groups of the pyridoxal moiety.

The EPR spectra were simulated[33] and the obtained spin Hamiltonian parameters g_z and A_z agree well with the values estimated using the additivity relationship proposed by Wüthrich[34] and Chasteen[32] with an estimated accuracy of $\pm 3 \times 10^{-4}$ cm^{-1}. The spin Hamiltonian parameters obtained by simulation of the experimental EPR spectra are included in Table 4, but for the donor groups under consideration their predicted contributions to the parallel hyperfine coupling constant are rather similar {for $O_{phenolate} \approx 38.9 \times 10^{-4}$ cm^{-1}; for N_{imine} $39 \pm 2 \times 10^{-4}$ cm^{-1}}.[33–38] Globally the hyperfine features of the spectra of **1**–**3** are consistent with a binding set that involves the $(O_{phenolate}, N_{imine}, N_{imine}, O_{phenolate})_{equatorial}$.

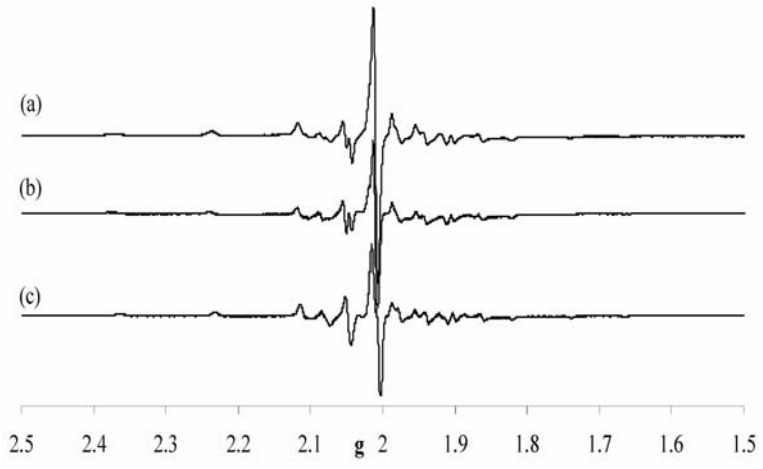

Figure 4. First-derivative EPR spectra of frozen (77 K) solutions of (a) [$V^{IV}O$(pydx-en)] (**1**) (4 mM) in MeOH; (b) [$V^{IV}O$(pydx-1,2-pn)] (**3**) (4 mM) in MeOH; and (**c**) [$V^{IV}O$(pydx-1,3-pn)] (**2**) (4 mM) in DMSO.

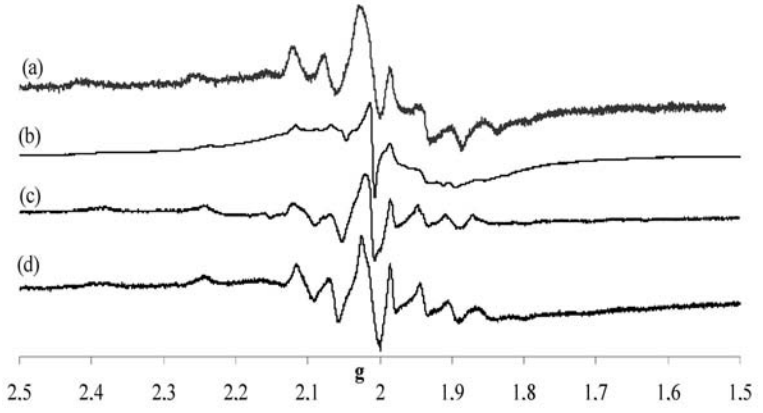

Figure 5. First-derivative EPR spectra at room temperature of zeolite-encapsulated complexes (solids) (a) [$V^{IV}O$]-Y; (b) [$V^{IV}O$(pydx-en)]-Y (**4**); (c) [$V^{IV}O$(pydx-1,2-pn)]-Y (**6**); (d) [$V^{IV}O$(pydx-1,3-pn)]-Y (**5**).

Table 4. Spin Hamiltonian parameters obtained[25] by simulation of the experimental EPR spectra.

Complex	Species	g_z	A_z [$\times 10^4$ cm^{-1}]	A_x, A_y [$\times 10^4$ cm^{-1}]	g_x, g_y
(**1**) 4 mM solution in MeOH		1.957	158.5	55.1	1.979
(**4**) solid	first species[a]	≈1.96	≈157	≈55	≈1.976
	second species[a]	≈1.96	≈159	≈60	≈1.975
(**2**) 4 mM solution in DMSO		1.956	156.6	48.3	1.985
(**5**) solid		≈ .95	≈166	≈59	≈1.981
(**3**) 4 mM solution in MeOH	first species	1.959	161.7	48	≈1.978
	second species	1.960	157.9	50	≈1.979
(**6**) solid		≈1.95	≈166	≈60	≈1.979

[a] Apparently, there are two species, but the corresponding A and g parameters given are only rough approximations of their correct values.

Hydrated zeolite-[$V^{IV}O$]-Y was previously reported and its EPR spectrum recorded.[39] It was concluded that the $V^{IV}O^{2+}$ ions are largely located on type-III sites in the large cavities bound to hydroxy or O atoms, the spin Hamiltonian parameters being as follows: g_z = 1.938 and A_z = 178×10^{-4} cm^{-1}. The EPR spectrum of the prepared zeolite-[$V^{IV}O$]-Y (Figure 5) shows rather broad lines, thus the spin Hamiltonian parameters cannot be determined accurately. They are $g_z \approx 1.939$ and $A_z \approx 176 \times 10^{-4}$ cm^{-1}, which is in good agreement with the data previously reported.[39]

As mentioned above, encapsulation of **1**–**3** in zeolite-Y involved the reaction of zeolite-[$V^{IV}O$]-Y with **I**, **II** or **III** in methanol, followed by careful and exhaustive extraction procedures to wash out any nonencapsulated vanadium species. Therefore we expect that all V^{IV} in compounds **4**–**6** corresponds to encapsulated complexes and no significant amount of complexes is bound to the external surface of the zeolite. The change of the EPR spectrum after introduction of a ligand and its similarity with the corresponding neat complex is thus good proof of the encapsulation of the $V^{IV}O$(ligand) species inside the pores of zeolite-Y.[1]

The EPR spectra recorded for **4**, **5** and **6** at 77 K also show relatively broad lines but differ from the spectrum of zeolite-[$V^{IV}O$]-Y used as precursor (Figure 5), thereby confirming the change in environment of the $V^{IV}O$ centre. As mentioned above, it is also probable that, besides the binding to the ligands, hydrogen-bond interactions are established between the zeolite–OH groups and the –CH_2OH and $N_{pyridine}$ moieties of the ligands. Equatorial or axial binding of zeolite–OH groups to $V^{IV}O$ is also possible and may explain the relatively high A_z values obtained for **5** and **6**. Notwithstanding, globally the EPR results for **4**–**6** confirm the presence of the $V^{IV}O$ complexes inside the nanopores of zeolite-Y and are consistent with their formulation as [$V^{IV}O$(pydx-en)]-Y (**4**), [$V^{IV}O$(pydx-1,3-pn)]-Y (**5**) and [$V^{IV}O$(pydx-1,2-pn)]-Y (**6**), each with a binding set $(O_{phenolate}, N_{imine}, N_{imine}, O_{phenolate})_{equatorial}$.

Catalytic Activity Studies

Oxidation of Styrene

To test the catalytic potential of the complexes prepared, the oxidation of styrene was chosen as one of the model reactions. Thus, the oxidation of styrene catalyzed by **4**–**6** was carried out using aqueous 30% H_2O_2 as an oxidant. It mainly gave styrene oxide, benzaldehyde, 1-phenylethane-1,2-diol, benzoic acid and phenylacetaldehyde along with only minor amounts of other unidentified products, as shown in Scheme 3.

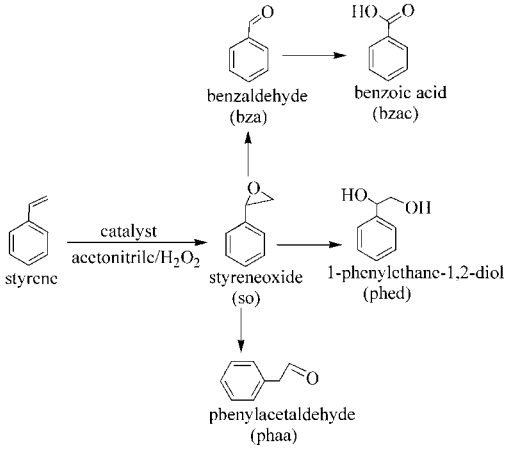

Scheme 3. Main products obtained upon the catalytic oxidation of styrene by the zeolite-encapsulated compounds **4**–**6**.

These products have also been observed when the polymer-supported complex PS-[VO(sal-ohyba)(dmf)] (H_2sal-ohyba = Schiff base derived from salicylaldehyde and *o*-hydroxybenzylamine; PS = polystyrene) was applied as catalyst.[40] These products of styrene oxidation were previously observed by others as well.[41–45]

In the present work, our objective was to achieve suitable reaction conditions for the maximum oxidation of styrene. Thus, [$V^{IV}O$(pydx-en)]-Y (**4**) was taken as a representative catalyst and different parameters, namely, the amount of oxidant (mol of H_2O_2 per mol of styrene), catalyst and temperature of the reaction mixture were tested.

For three different molar ratios of styrene to aqueous 30% H_2O_2 (e.g., 1:1, 1:2 and 1:3), the amount of styrene (1.04 g, 10 mmol) and catalyst (0.010 g) were taken in CH_3CN (5 mL), and the reaction was carried out at 80 °C. The formation of products was regularly analyzed at similar time intervals. As illustrated in Figure 6, increasing the H_2O_2/styrene ratio from 1:1 to 2:1 improved the conversion from around 60 to 86%. The oxidation improved only marginally upon further increasing this ratio to 1:3, which suggested that a higher amount of oxidant does not improve the oxidation of styrene, a 1:2 ratio being considered adequate.

Similarly, for three different amounts (that is, 0.005, 0.010 and 0.015 g) of catalyst for the fixed amount of styrene (1.04 g, 10 mmol), H_2O_2 (2.28 g, 20 mmol), CH_3CN (5 mL) and temperature (80 °C), 0.005 g of catalyst gave only 64.4% conversion (Figure 7). A maximum of 85.5%

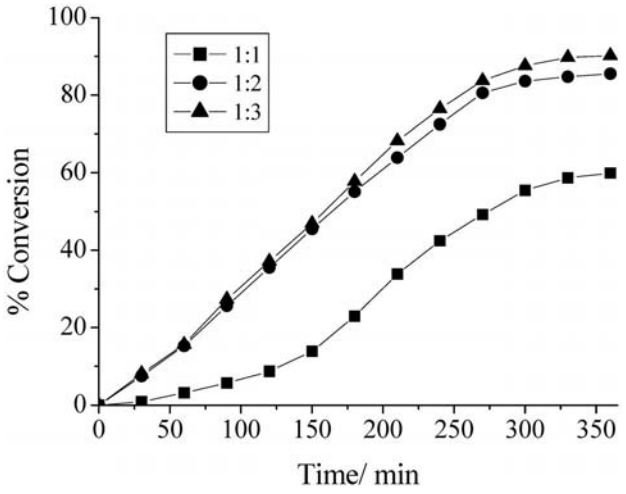

Figure 6. Effect of the amount of H_2O_2 on the oxidation of styrene at 80 °C as a function of time. Reaction conditions: styrene (1.04 g, 10 mmol), [$V^{IV}O$(pydx-en)]-Y (0.010 g), acetonitrile (5 mL).

conversion was achieved upon increasing the amount to 0.010 g, whereas further increments of catalyst amount resulted in lower conversion. Therefore, an amount of 0.010 g of catalyst may be considered adequate to obtain the maximum conversion of styrene. The temperature of the reaction mixture also influenced the performance of the catalyst; running the reaction at 80 °C gave much better conversion than at lower temperatures and also reduced the time required to achieve the maximum conversion.

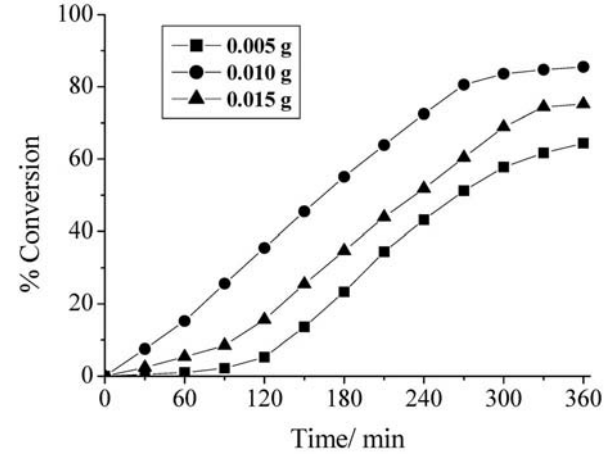

Figure 7. Effect of the amount of catalyst on the oxidation of styrene at 80 °C as a function of time. Reaction conditions: styrene (1.04 g, 10 mmol), H_2O_2 (2.27 g, 20 mmol) in acetonitrile (5 mL).

Interestingly 5 mL of acetonitrile was found to be sufficient to effect maximum oxidation of styrene, with significantly lower conversions being observed with 10 or 15 mL (Figure 8). This is probably due to a much higher concentration gradient of reagents between the outside and inside of the zeolite cavities when the volume of solvent is lower, thus emphasizing the important role of mass transfer in reactions that involve catalysts encapsulated in zeolite-Y. As the net amount of oxidant is the same, the H_2O_2 concentration is also higher when the volume of solvent added is lower.

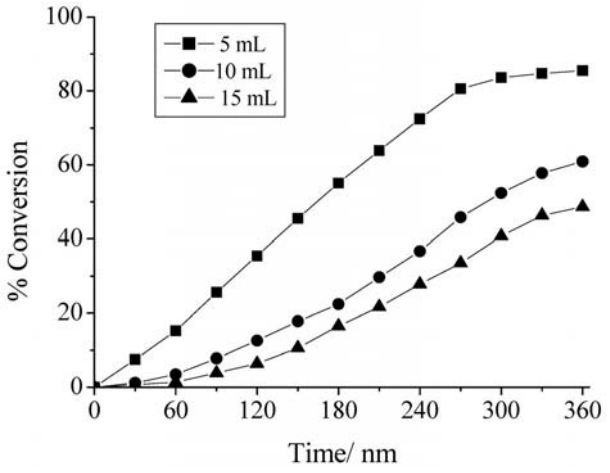

Figure 8. Effect of the amount of solvent on the oxidation of styrene at 80 °C as a function of time. Reaction conditions: styrene (1.04 g, 10 mmol), H_2O_2 (2.27 g, 20 mmol), [$V^{IV}O$(pydx-en)]-Y (0.010 g).

Thus, for the maximum oxidation of 10 mmol of styrene, the following conditions were considered an adequate balance: catalyst (0.010 g, around 3.5 μmol of V complex), H_2O_2 (2.27 g, 20 mmol), CH_3CN (5 mL) and reaction temperature (80 °C). The other catalyst precursors, [$V^{IV}O$-(pydx-1,3-pn)]-Y and [$V^{IV}O$(pydx-1,2-pn)]-Y, were also tested under the above optimized reaction conditions (Figure S2 in the Supporting Information), and the results are presented in Table 5. It is clear from the data that all catalysts give comparable conversion and selectivity. This observation confirms that chain length of the amine residue does not have a relevant influence on the performance of the catalyst. Probably the critical issue in the present encapsulated catalysts **4**–**6** is the mass transfer of reagents and/or products in and out of the zeolite cages, and the differences in the calculated time of flight (TOF) values between **4**, **5** and **6** do not really represent relevant differences in their catalytic activities, but instead result from the distinct amount of complex present inside the zeolite cavities in **4**, **5** and **6**, which leads to distinct calculated TOF values.

The conversion of styrene and the selectivity of different reaction products using [$V^{IV}O$(pydx-en)]-Y as catalyst under the optimized reaction conditions have been analyzed as a function of time and are presented in Figure 9. It is clear from the plot that a selectivity of 75.5% of benzaldehyde has been obtained at a conversion of 7.5% of styrene in 0.5 h of reaction time. This selectivity slightly improves in the first two hours, then slowly decreases with time and reaches 74.7% with the increase of the conversion of styrene to 85.5% in 6 h. With 24.5% at a reaction time of 0.5 h, the selectivity of styrene oxide decreases considerably with the conversion of styrene and reaches 3.9%. The formation of the other three products (i.e., benzoic acid, 1-phenylethane-

Table 5. Percentage conversion of styrene, product selectivity and turn over frequency (TOF).

Catalyst	Conv. [%]	TOF [h^{-1}][b]	Selectivity[c] [%]					
			so	bza	phed	bzac	phaa	other
[V^{IV}O(pydx-en)]-Y (**4**)	85.5	490[d]	3.9	74.7	9.4	6.8	3.4	1.8
[V^{IV}O(pydx-en)]-Y[a]	83.4	–	3.7	72.7	9.1	7.2	5.0	2.3
[V^{IV}O(pydx-1,3-pn)]-Y (**5**)	84.6	466[d]	4.1	74.1	9.3	6.1	2.9	3.5
[V^{IV}O(pydx-1,3-pn)]-Y[a]	83.2	–	3.5	73.2	8.6	5.6	6.4	3.7
[V^{IV}O(pydx-1,2-pn)]-Y (**6**)	82.9	553[d]	3.8	76.5	8.2	5.8	2.0	3.6
[V^{IV}O(pydx-1,2-pn)]-Y[a]	81.7	–	3.3	75.4	8.0	7.7	2.7	3.9
[V^{IV}O]-Y	4.8	–	–	75.0	–	25.0	–	–
[V^{IV}O(pydx-en)] (**1**)	65.3	369[e]	2.3	74.8	4.1	10.6	3.4	4.8
[V^{IV}O(pydx-1,2-pn)] (**3**)	62.7	366[e]	2.6	73.8	3.4	10.2	4.8	5.2
[V^{IV}O(pydx-1,3-pn)] (**2**)	63.2	369[e]	1.8	74.5	3.6	9.6	6.7	3.7

[a] First cycle of used catalyst after recycling. [b] TOF values calculated at 5 h of reaction time. [c] so: styrene oxide, bza: benzaldehyde, phed: 1-phenylethane-1,2-diol, bzac: benzoic acid, phaa: phenyl acetaldehyde. [d] The different TOF values mostly reflect the distinct amount of V^{IV} present in 0.010 g of catalysts **4**–**6** (see Table 1): ≈3.5 μmol (**4**), ≈3.6 μmol (**5**) and ≈2.9 μmol (**6**). [e] The amounts of catalysts in 0.0015 g of catalysts are ≈3.5 μmol (**1**), ≈3.4 μmol (**2**) and ≈3.4 μmol (**3**).

1,2-diol and phenyl acetaldehyde) starts only after approximately 2 h, and their overall formation is relatively low even after 6 h of the reaction time.

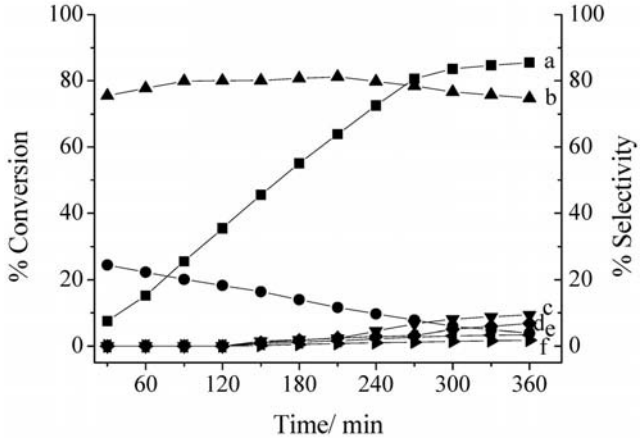

Figure 9. Conversion of styrene and variation in the selectivity of different reaction products as a function of time using [V^{IV}O(pydx-en)]-Y as catalyst: (a) conversion of styrene (filled square), (b) selectivity of benzaldehyde (filled triangle), (c) selectivity of 1-phenylethane-1,2-diol (filled upside-down triangle), (d) selectivity of benzoic acid (filled diamond), (e) selectivity of styrene oxide (filled circle), (f) selectivity of other products (filled triangle to left).

It is clear from Table 5 that the selectivity of the different oxidation products formed varies in the order: benzaldehyde >> 1-phenylethane-1,2-diol > benzoic acid > styrene oxide > phenylacetaldehyde. Upon recycling, the overall results are very similar: the activity decreases slightly and the selectivity shows small changes, with an increase in the formation of phenylacetaldehyde and of the minor unidentified products.

Neat complexes **1**–**3** are also active and exhibit 62.7–65.3% conversion (Table 5) with rather similar selectivity. However, the selectivity of the products differs between encapsulated and nonencapsulated catalysts. Indeed, the selectivity for the most relevant product, benzaldehyde, is approximately the same, but the relative amount of benzoic acid is higher and that of 1-phenylethane-1,2-diol is lower, whereas others follow a similar order of selectivity to that observed for encapsulated complexes. A blank reaction under the above reaction conditions gave around 3% conversion. Thus, neat as well as encapsulated complexes show good performance, but the catalytic activity is significantly higher in the case of the encapsulated complexes **4**–**6**. In addition to the easier hydrolysis of the neat complexes **1**–**3** in the presence of aqueous H_2O_2 relative to their encapsulated counterparts, it is possible that these may also form oligomeric inactive species.[31] Therefore, besides their higher activity, the recyclable nature, higher stability and no observed leaching of encapsulated complexes make them significantly better over the neat ones.

Aspects related to the mechanism of reaction are discussed below. Benzaldehyde is clearly the favoured product. It may result from the further oxidation of styrene oxide formed in the first step by a nucleophilic attack of H_2O_2 on styrene oxide followed by cleavage of the intermediate hydroperoxystyrene.[1] The formation of benzaldehyde may also result from direct oxidative cleavage of the styrene side-chain double bond through a radical mechanism. The high amount of water present in H_2O_2 is partly responsible for the possible hydrolysis of styrene oxide to 1-phenylethane-1,2-diol (phed). It is plausible that relatively high amounts of H_2O adsorb onto the zeolite surface, namely, inside the pores, which would explain why phed forms in higher amounts in the case of the zeolite-encapsulated catalysts **4**–**6** relative to **1**–**3**. Other products (e.g., benzoic acid formation through further oxidation of benzaldehyde) only form in relatively low amounts in these reactions, although significantly higher in the case of reactions that involve neat complexes **1**–**3** as catalysts. Similarly, the formation of phenylacetaldehyde through isomerization of styrene oxide is quite low in all cases.

Oxidation of Cyclohexene

The oxidation of cyclohexene was also studied using these catalysts. The reaction gave mainly four different products, that is, 2-cyclohexen-1-ol, 2-cyclohexen-1-one and cyclohexane-1,2-diol, as shown in Scheme 4. The formation

of the allylic oxidation products 2-cyclohexen-1-one and 2-cyclohexen-1-ol reflects the preferential attack of the activated C–H bond over the C=C bond.[46]

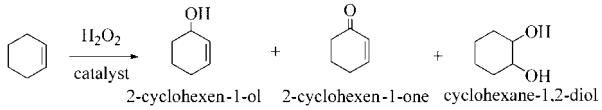

Scheme 4. Oxidation products of cyclohexene.

The different parameters (e.g., amount of oxidant, catalyst, solvent and temperature of the reaction mixture) were optimized for the maximum oxidation of cyclohexene, again considering [$V^{IV}O$(pydx-en)]-Y (**4**) as a representative catalyst. Three different molar ratios of cyclohexene to aqueous 30% H_2O_2 (e.g., 1:1, 1:2 and 1:3) were considered while keeping fixed the amounts of cyclohexene (0.082 g, 10 mmol), catalyst precursor (0.005 g), acetonitrile (5 mL) and temperature at 80 °C. The percent conversion obtained as a function of time is presented in Figure 10. A maximum of 90.4% conversion was achieved at an cyclohexene-to-H_2O_2 molar ratio of 1:1. Increasing this ratio to 1:2 increased this conversion to 95.9%, whereas 1:3 molar ratios gave 96.9% conversion (Figure 10). As the 1:3 molar ratio of substract/oxidant did not show significant change in the conversion of cyclohexene, the cyclohexene-to-H_2O_2 molar ratio of 1:2 was considered to be adequate.

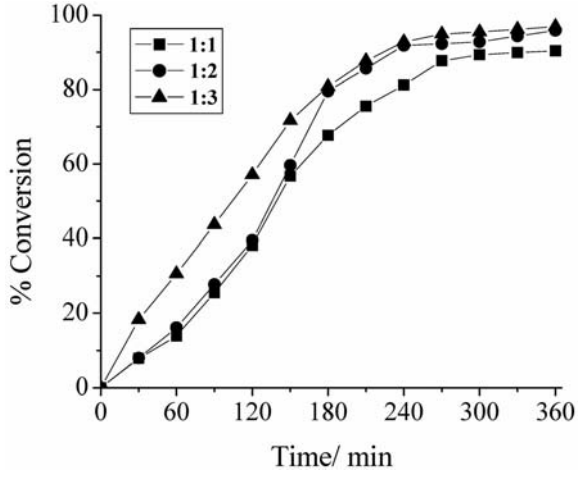

Figure 10. Effect of the amount of H_2O_2 on the oxidation of cyclohexene at 80 °C as a function of time. Reaction conditions: cyclohexene (0.820 g, 10 mmol), [$V^{IV}O$(pydx-en)]-Y (0.005 g) and acetonitrile (5 mL).

Similarly, for cyclohexene (0.082 g, 10 mmol), 30% H_2O_2 (2.27 g, 20 mmol) and acetonitrile (5 mL), three different amounts of catalyst (e.g., 0.003, 0.005 and 0.0075 g) were considered and the reactions were monitored at 80 °C. The results obtained as a function of time are presented in Figure S3 in the Supporting Information; they indicate that 0.005 g of catalyst amount shows a maximum conversion of 95.9%, whereas 0.003 and 0.0075 g of catalyst gave lower conversions (around 76 and 80%, respectively) in 5–6 h of reaction time.

As illustrated in Figure 11, under the above optimized reaction conditions {i.e., cyclohexene (0.82 g, 10 mmol), [$V^{IV}O$(pydx-en)]-Y (0.005 g) and H_2O_2 (2.27 g, 20 mmol) in 5 mL of acetonitrile} are adequate to effect 95.9% conversion of cyclohexene at 80 °C. Remarkably, increasing the solvent volume decreases this conversion drastically.

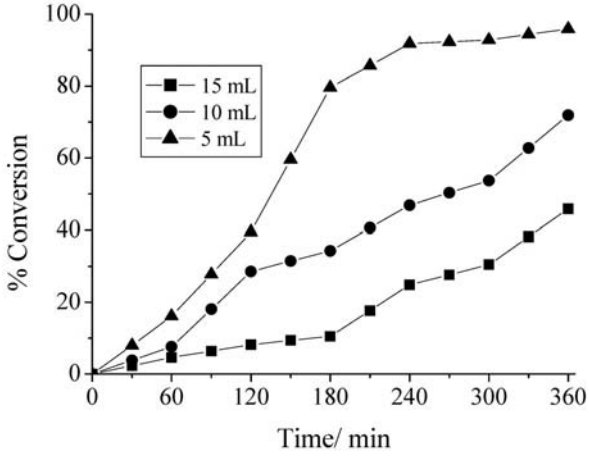

Figure 11. Effect of the amount of solvent on the oxidation of cyclohexene at 80 °C as a function of time. Reaction conditions: cyclohexene (0.82 g, 10 mmol), H_2O_2 (2.27 g, 20 mmol) and [$V^{IV}O$-(pydx-en)]-Y (0.005 g).

Thus, under the optimized conditions [i.e., cyclohexene (0.82 g, 10 mmol), H_2O_2 (2.27 g, 20 mmol), catalyst (0.005 g) CH_3CN (5 mL) and temperature (80 °C)], the performance of catalyst precursors **5** and **6** and of **1**–**3** was also studied. The conversions after 4–6 h of reaction time (Figure S4 in the Supporting Information) along with the product selectivity after 6 h are presented in Table 6. The activity of **2** is higher than that of **1** and **3**, but this trend is not preserved in their encapsulated counterparts.

Again the catalytic activity of the encapsulated complexes is significantly higher than their neat counterparts due to more extensive hydrolysis and/or formation of inactive oligomeric species in the presence of aqueous H_2O_2. It is also probable in the present reaction that mass transfer in, out and within the zeolite pores determines the kinetics of the whole catalytic process and that the TOF values for **4**–**6** do not particularly reflect the different catalytic activities between **4**, **5** and **6**; instead they mostly result from the different amount of catalyst inside the pores of **4**–**6**. Therefore we conclude that the catalytic performance of all encapsulated catalysts is comparable for the oxidation of cyclohexene. The selectivity of the products follows the order: 2-cyclohexen-1-one > 2-cyclohexen-1-ol > cyclohexane-1,2-diol > cyclohexene oxide. After approximately 4 h, the conversion has almost attained its maximum and only increases marginally between 4 and 6 h of reaction time. Neat complexes exhibit much lower conversion along with lower turn over frequency (Table 6). Here, the selectivity of different products also differs and follows the order: 2-cyclohexen-1-ol >> 2-cyclohexen-1-one > cyclohexene oxide > cyclohexane-1,2-diol.

Table 6. Conversion of cyclohexene and selectivity of various oxidation products after 6 h of reaction time.

Catalyst	Conv. [%]	TOF [h^{-1}]	Selectivity[b] [%] a	b	c	d	others
[$V^{IV}O$(pydx-en)]-Y (**4**)	95.9	1374[c]	1.6	32.9	50.8	9.7	4.9
[$V^{IV}O$(pydx-en)]-Y[a]	94.2	–	2.8	51.6	43.0	1.6	1.0
[$V^{IV}O$(pydx-1,3-pn)]-Y (**5**)	92.6	1276[c]	2.5	43.9	46.7	3.9	2.9
[$V^{IV}O$(pydx-1,3-pn)]-Y[a]	90.4	–	3.0	45.4	35.1	13.4	3.1
[$V^{IV}O$(pydx-1,2-pn)]-Y (**6**)	89.2	1487[c]	2.8	42.9	50.2	3.3	0.1
[$V^{IV}O$(pydx-1,2-pn)]-Y[a]	85.8	–	3.0	47.8	35.0	10.9	3.3
Without catalyst	6.6	–	49.4	10.0	25.0	15.6	–
[$V^{IV}O$(pydx-en)] (**1**)	28.1	595[d]	9.4	66.8	21.0	2.8	–
[$V^{IV}O$(pydx-1,3-pn)] (**2**)	32.2	704[d]	5.9	57.3	32.7	4.2	–
[$V^{IV}O$(pydx-1,2-pn)] (**3**)	23.1	505[d]	10.9	59.1	24.2	5.7	–

[a] First cycle of used catalyst after recycling. [b] (a) cyclohexene oxide, (b) 2-cyclohexen-1-ol, (c) 2-cyclohexen-1-one and (d) cyclohexane-1,2-diol. [c] The different TOF values mainly reflect the distinct amount of V^{IV} present in 0.005 g of catalysts **4**–**6** (see Table 1): ca. 1.75 μmol (**4**), ca. 1.8 μmol (**5**) and ca. 1.45 μmol (**6**). [d] The amounts of catalysts in 0.0010 g of catalysts are ca. 2.4 μmol (**1**), ca. 2.3 μmol (**2**) and ca. 2.3 μmol (**3**).

The conversion of cyclohexene and the selectivity of different reaction products using [VO(pydx-en)]-Y (**4**) as catalyst under the optimized reaction conditions have been analyzed as a function of time and are presented in Figure 12. The formation of 2-cyclohexen-1-ol started with a selectivity of approximately 60% which slowly decreased with time and reached around 33.6% at the end of 6 h of reaction. Similarly, the selectivity of cyclohexene oxide started with 17.3% and reached 1.6%, whereas 2-cyclohexen-1-one started with around 36% selectivity and improved to around 54.6%. The formation of cyclohexane-1,2-diol was initially nearly zero and increased up to 9.8% after 6 h. The other catalysts gave similar selectivity trends.

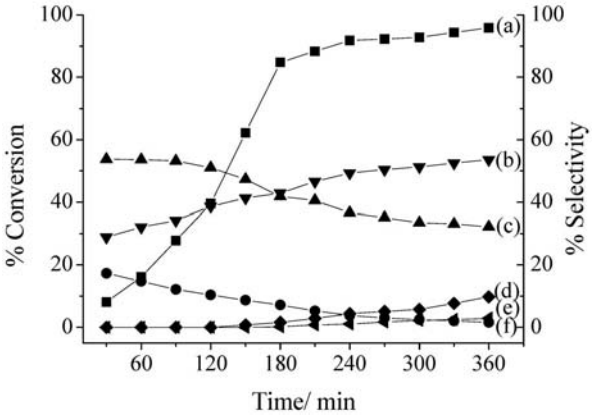

Figure 12. Conversion of cyclohexene and variation in the selectivity of the different reaction products as a function of time using [$V^{IV}O$(pydx-en)]-Y (**4**) as catalyst: (a) conversion of cyclohexene (filled square), (b) selectivity of cyclohexen-1-one (filled inverted triangle), (c) selectivity of cyclohexen-1-ol (filled triangle), (d) selectivity of cyclohexane-1,2-diol (filled diamond) (e) selectivity of cyclohexene oxide (filled circle) and (f) selectivity of other products (filled triangle to left).

Oxidation of Methyl Phenyl Sulfide (Thioanisole)

Several vanadium-dependent haloperoxidases catalyze sulfoxidations[47–49] in which the electron-rich sulfur atom of the sulfide undergoes electrophilic oxidation by H_2O_2 to give the sulfoxide and, further, sulfone. Such oxidation of methyl phenyl sulfide was tested with the precursor catalysts (i.e., $V^{IV}O$ complexes encapsulated in the nanocavities of zeolite-Y). Oxidation of methyl phenyl sulfide in the presence of H_2O_2 gave two products: methyl phenyl sulfoxide and methyl phenyl sulfone, as shown in Scheme 5.

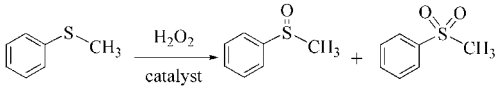

Scheme 5. Oxidation of organic sulfides.

Among the three encapsulated complexes studied, [$V^{IV}O$-(pydx-en)]-Y (**4**) was chosen again as a representative one and the reaction conditions were optimized by considering the amount of catalyst precursor, oxidant and solvent to obtain maximum conversion of thioanisole. The effect of H_2O_2 was studied by considering substrate-to-oxidant ratios of 1:1, 1:2 and 1:3 for the fixed amount of catalyst (0.010 g) and methyl phenyl sulfide (1.242 g, 10 mmol) in acetonitrile (5 mL) and the reaction was monitored at room temperature (Figure S5 in the Supporting Information). At an aqueous H_2O_2/substrate ratio of 2:1, a maximum of 85.5% conversion of methyl phenyl sulfide was achieved in 2.5 h of reaction time. Decreasing this ratio to 1:1 decreased the conversion of methyl phenyl sulfide considerably, whereas increasing this ratio to 3:1 improved the conversion but not much (Figure S5), and it facilitated the reaction to achieve equilibrium in a shorter time. However, an aqueous H_2O_2/substrate ratio of 2:1 may be considered adequate to obtain maximum conversion of methyl phenyl sulfide.

Similarly, three different amounts of catalyst precursors, that is, 0.005, 0.010 and 0.015 g, were taken while keeping methyl phenyl sulfide (1.242 g, 10 mmol) and 30% H_2O_2 (2.27 g, 20 mmol) in acetonitrile (5 mL) to check the effect of amount of catalyst on the reaction. As may be seen in Figure S6 in the Supporting Information, increasing its amount from 0.005 g to 0.010 g increased the conversion from 82.4 to 85.5%, whereas 0.015 g of catalyst gave a marginal increase to 87.0% conversion. Thus, 0.010 g of catalyst precursor is adequate to obtain an optimum methyl

phenyl sulfide conversion of 85.5% in around 2.5 h of contact time.

In this reaction, the volume of solvent again has a remarkable role in the oxidation of methyl phenyl sulfide. As may be seen in Figure 13, the use of 5 mL of acetonitrile gave much better conversion under above optimized reaction conditions of catalyst and oxidant than 10 or 15 mL. This may possibly be due to a much higher concentration gradient of reagents between the outside and inside of the zeolite cavities when the volume of solvent is lower.

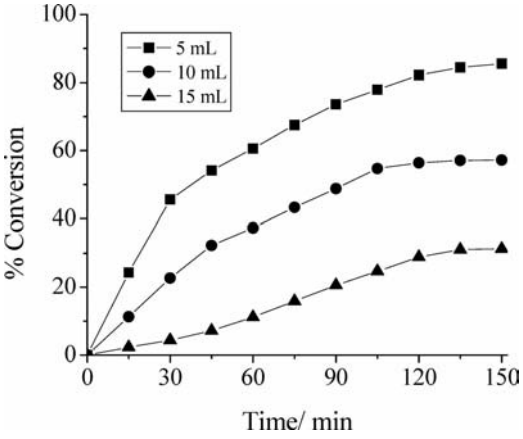

Figure 13. Effect of volume of solvent on the oxidation of methyl phenyl sulfide at room temperature as a function of time. Reaction conditions: methyl phenyl sulfide (1.242 g, 10 mmol), H_2O_2 (2.2 g, 20 mmol) and [V^{IV}O(pydx-en)]-Y (0.010 g).

Therefore, from these experiments, the more adequate reaction conditions for the maximum oxidation of methyl phenyl sulfide at room temperature are considered to be: catalyst (0.010 g), methyl phenyl sulfide (1.242 g, 10 mmol), H_2O_2 (2.27 g, 20 mmol) and acetonitrile (5 mL). The other catalyst precursors **5** and **6** were also tested under the above reaction conditions. The corresponding results are summarized in Figure S7 in the Supporting Information and selectivity details are presented in Table 7.

From Table 7, it is clear that 80.0–85.5% of methyl phenyl sulfide is converted into products using all catalysts for which the percentage conversion varied in the order: [V^{IV}O(pydx-en)]-Y (85.5%) > [V^{IV}O(pydx-1,3-pn)]-Y (82.1%) > [V^{IV}O(pydx-1,2-pn)]-Y (80.0%). The selectivity of the major product (i.e., sulfone) is similar but varies in the order: [V^{IV}O(pydx-en)]-Y (79.6%) > [V^{IV}O(pydx-1,3-pn)]-Y (75.2%) > [V^{IV}O(pydx-1,2-pn)]-Y (73.6%).

The conversion of methyl phenyl sulfide and the selectivity of different reaction products using **4** as catalyst under the optimized reaction conditions were obtained as a function of time and are presented in Figure 14. It is clear from the plot that conversion of methyl phenyl sulfide starts with the good selectivity (around 90%) for the formation of methyl phenyl sulfoxide, but this is slowly converted into the sulfoxide. The initial selectivity of methyl phenyl sulfone is around 10% and reaches around 20% after around 2.5 h. Very similar trends were also obtained with the catalyst precursors **5** and **6**.

Table 7. Conversion percentage of methyl phenyl sulfide in 2.5 h and selectivity of sulfoxide and sulfone.

Catalyst	Conv. [%]	TOF [h^{-1}]	Selectivity [%] sulfoxide	sulfone
[V^{IV}O(pydx-en)]-Y (**4**)	85.5	980[c]	79.6	20.4
[V^{IV}O(pydx-en)]-Y[a]	83.5	–	75.7	24.3
[V^{IV}O(pydx-1,3-pn)]-Y (**5**)	82.1	905[c]	75.2	24.8
[V^{IV}O(pydx-1,3-pn)]-Y[a]	80.4	–	73.2	26.8
[V^{IV}O(pydx-1,2-pn)]-Y (**6**)	80.0	1067[c]	73.6	26.4
[V^{IV}O(pydx-1,2-pn)]-Y[a]	77.8	–	73.4	26.6
No solid[b]	≈3	–	≈3	≈0
Na–Y[b]	≈3	–	≈3	≈0
[V^{IV}O(pydx-en)] (**1**)	80.3	906	82.5	17.5
[V^{IV}O(pydx-1,2-pn)] (**3**)	75.8	884	80.8	19.2
[V^{IV}O(pydx-1,3-pn)] (**2**)	78.5	916	81.3	18.7

[a] First cycle of used catalyst. [b] 10 mL of acetonitrile. [c] The different TOF values mainly reflect the distinct amount of V^{IV} present in 0.005 g of catalysts **4**–**6** (see Table 1): ca. 3.5 μmol (**4**), ca. 3.6 μmol (**5**) and ca. 2.9 μmol (**6**). [d] The amounts of catalysts in 0.0015 g of catalysts are ca. 3.5 μmol (**1**), ca. 3.4 μmol (**2**) and ca. 3.4 μmol (**3**).

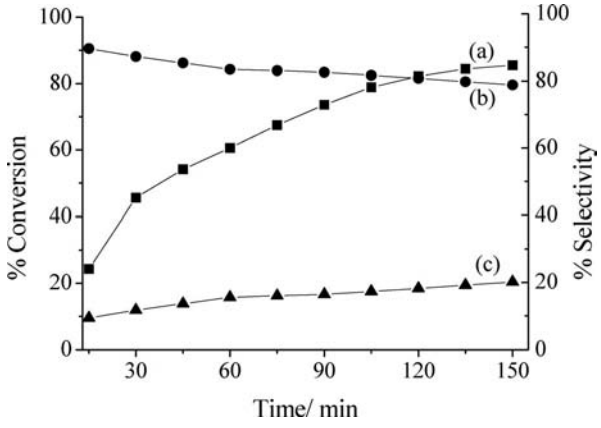

Figure 14. Conversion of methyl phenyl sulfide and variation in the selectivity of the reaction products as a function of time using **4** as catalyst: (a) conversion of methyl phenyl sulfide (filled circle), (b) selectivity of methyl phenyl sulfoxide (filled square) and (c) selectivity of methyl phenyl sulfone (filled triangle).

Considering the same molar concentration of neat catalyst precursors [V^{IV}O(pydx-en)] (**1**), [V^{IV}O(pydx-1,3-pn)] (**2**) and [V^{IV}O(pydx-1,2-pn)] (**3**) under reaction conditions approximately equivalent to those above [i.e., catalyst (0.001 g for all), methyl phenyl sulfide (1.242 g, 10 mmol), H_2O_2 (2.27 g, 20 mmol) and acetonitrile (5 mL)], 75.8–80.3% conversion of methyl phenyl sulfide was achieved after 2.5 h for which selectivity of sulfoxide was around 82%, which is slightly higher than obtained for the encapsulated complexes. It is possible that the local polar environment inside the zeolite pores, which favours hydrogen-bond formation and adsorption of H_2O and H_2O_2, may explain the higher degree of oxidation of the sulfide in the case of catalysts **4**–**6**. Globally both neat as well as encapsulated complexes may be considered as good catalysts for the oxidation of the organic sulfide; however, the stability and recyclable nature of zeolite-Y-encapsulated complexes make them better over neat ones.

Tests of Recyclability and Heterogeneity of the Zeolite-Y-Encapsulated Catalytic Reactions

The recyclability of encapsulated complexes was examined by considering the oxidation of styrene. After contact for 6 h, the reaction mixture was filtered, and the solid was washed with acetonitrile and dried at approximately 120 °C. It was subjected to further catalytic reaction under similar conditions. As may be seen in Table 5, not much loss in catalytic activity was observed, thus indicating that most of the complex is still present in the cavity of the zeolite-Y. In another experiment, after approximately 6 h of reaction time, the filtrate collected after separating the used catalyst was placed into the reaction flask and the reaction was continued for another 4 h after adding fresh oxidant. The gas chromatographic analysis showed no significant improvement in conversion, and this confirms that the reaction did not proceed upon removal of the solid catalyst. The oxidation of styrene is therefore heterogeneous in nature, and no leaching of the active complex occurred during the catalytic cycle. Similar experiments were done for the oxidation of cyclohexene (Table 6) and methyl phenyl sulfide (Table 7). The recycle experiments for cyclohexene show not much loss in catalytic activity, whereas in the case of methyl phenyl sulfide it gave around 2% less conversion than the original catalyst.

Reactivity of Complexes and Possible Catalytic Reaction Pathway

It is known that several $V^{V}O_2$**L** compounds react with H_2O_2 to give $V^{V}O(O_2)$**L**, and it is normally assumed that the corresponding hydroperoxido complex is the active catalyst that mediates oxygenations, including the oxidation of sulfides to sulfoxides and sulfones as well as the epoxidation of alkenes and allylic alcohols.[50]

The reactivity of $[V^{IV}O(pydx\text{-}en)]$ with H_2O_2 in DMSO was monitored by electronic absorption spectroscopy. The observed spectral changes are presented in Figure 15. Thus, the progressive addition of a dilute H_2O_2 solution in DMSO to a solution of $[V^{IV}O(pydx\text{-}en)]$ in DMSO results in the flattening of bands that appear at 776 and 650 nm. The intensity of the band at around 385 nm slowly decreases with a slight shift towards lower wavelength and stabilizes with the formation of a band at around 380 nm, whereas the intensity of other bands that appear in the UV region (at around 260 and around 280 nm) increases. These changes indicate the interaction of $[V^{IV}O(pydx\text{-}en)]$ with H_2O_2 in methanol, thus forming $[V^{V}O(O)_2(pydx\text{-}en)]$, for

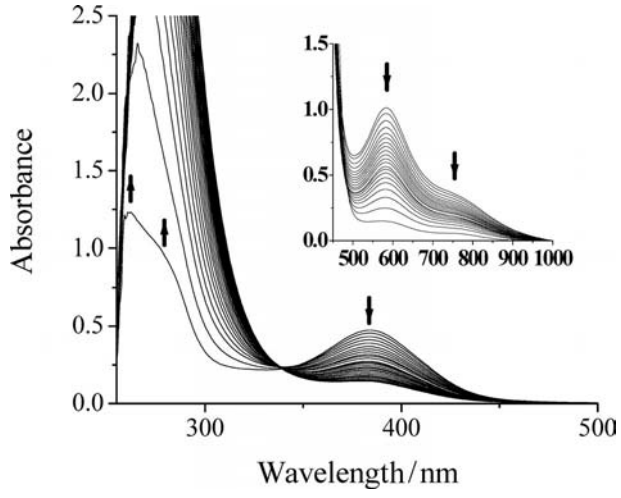

Figure 15. UV/Vis spectral changes observed during titration of $[V^{IV}O(pydx\text{-}en)]$ (**1**) with H_2O_2. The spectra were recorded upon stepwise additions of five drops portions of H_2O_2 [1.178 g (10.39 mmol) of 30% H_2O_2 dissolved in 5 mL of DMSO] to 10 mL of 1.6×10^{-4} M solution in DMSO. The inset shows similar spectra recorded with around 7.55×10^{-3} M solution of **1** in DMSO.

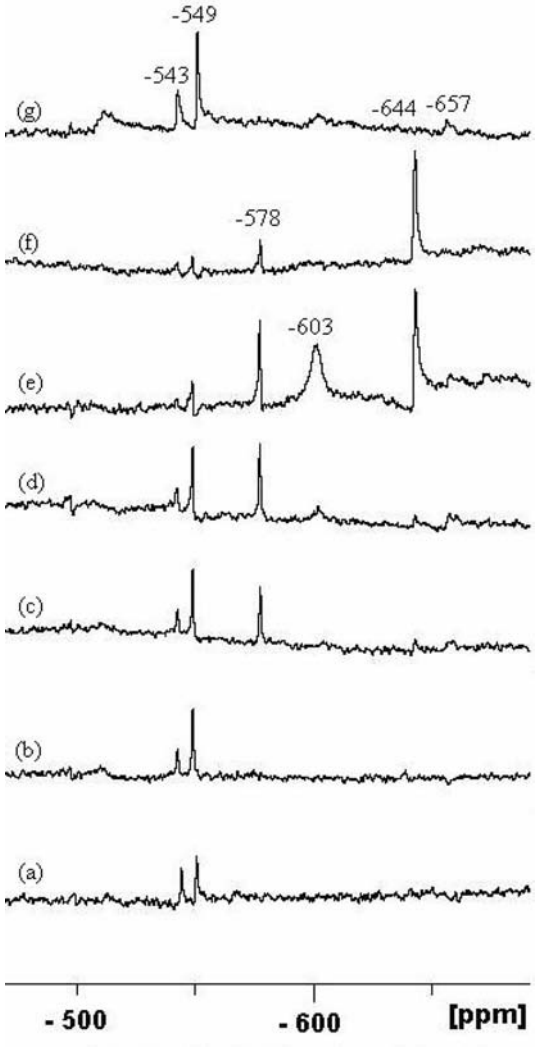

Figure 16. ^{51}V NMR spectra (a) of a solution of $[V^{IV}O(pydx\text{-}en)]$ (**1**) (ca. 4 mM) in methanol; the pH is around 7.5; (b) solution of (a) after 1 h; (c) addition of 0.5 equiv. of aqueous 30% H_2O_2 (total) to the solution of (b); (d) after addition of 1.0 equiv. of 30% H_2O_2 (total) to the solution of (c); (e) after addition of 2.0 equiv. of 30% H_2O_2 (total) to the solution of (d) the pH is around 6.5; (f) after addition of 3.0 equiv. (30%) H_2O_2 (total) to the solution of (e) the pH is around 6.5; (g) addition of methyl phenyl sulfide (10 equiv.) to the solution of (f) after 3h at room temperature.

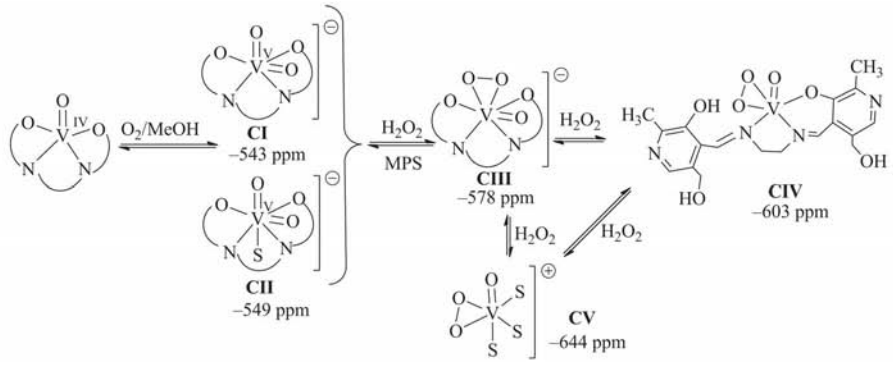

Scheme 6. Tentative assignments of V^V species formed in methanolic solutions of [$V^{IV}O$(pydx-en)] (**1**), upon addition of aqueous H_2O_2 solution, and upon addition of methyl phenyl sulfide. The tetradentate ligand is schematically represented as O–N–N–O for most of the V^{IV} or V^V species presented. ^{51}V NMR spectroscopic assignments are partly based on results reported for other systems[24,40] upon addition of aqueous H_2O_2.

which bands at around 360–450 nm are expected to appear (see ref.[40] and references cited therein). The disappearance of d–d bands is in accordance with the oxidation of the $V^{IV}O$ to V^V complexes.

Similar features were observed with [$V^{IV}O$(pydx-1,2-pn)] upon similar treatment (Figure S8 in the Supporting Information).

The ^{51}V NMR spectra of [$V^{IV}O$(pydx-en)] (**1**) were recorded to establish their behaviour in solution and their speciation upon modifying the composition of the solutions (see Figure 16). A fresh solution of [$V^{IV}O$(pydx-en)] (**1**) (around 4 mM) in methanol does not show any ^{51}V NMR spectroscopic peak. But after approximately 15 min, resonances at δ = –543 and –549 ppm build up, which we tentatively assign to species **CI** and **CII** (see Scheme 6). Upon successive additions of portions of a 30% H_2O_2 aqueous solution, the relative intensity of the δ = –543 and –549 ppm peaks decrease and several new peaks build up. Namely, after addition of around 0.5 equiv. of H_2O_2, a peak at δ = –578 ppm emerges; it corresponds to the monoperoxido **CIII**, and upon further additions (1.0, 2.0 and 3.0 equiv.) of the 30% H_2O_2 solution, new peaks appear at δ = –603 (**CIV**) and –644 (**CV**), which increase intensity at the expense of the resonances of **CI** and **CII**. Upon addition of methyl phenyl sulfide (MPS), after around 3 h the peaks at δ = –644 and –578 ppm that correspond to the peroxide complexes **CIII** and **CIV** disappear and the spectrum (Figure 16g) shows the resonances at δ = –543 and –549 ppm that correspond to **CI** and **CII** as the main peaks.

These results indicate that during the catalytic reactions by peroxide, intermediate peroxido species indeed form. Upon addition of methyl phenyl sulfide, the oxidant is consumed and the catalytic precursors [V^VO_2(pydx-en)$(S)_n$] (n = 0, 1) are restored. The EPR spectra measured (Figure S9 in the Supporting Information) indicate that this solution also contains [$V^{IV}O$(pydx-en)] (**1**).

Thus, overall these UV/Vis and ^{51}V NMR spectroscopic experiments show that upon addition of aqueous H_2O_2, $V^VO(O)_2$**L** species form, thereby supporting the possibility of hydroperoxide complexes being the active catalyst. After addition of the substrate (e.g., methyl phenyl sulfide) both V^V and V^{IV}-**L** complexes are the only V-containing species detected, thus indicating that the integrity of the ligand is preserved or may be restored after the oxidant is consumed. Thus, recyclability of the catalyst precursors mainly depends on the more or less easy separation of the complex from the reaction mixture that contains the products.

We recently reported the catalytic oxidation of styrene by [V^VO_2(pydx-aebmz)] (**7**) and [V^VO_2(pydx-ambmz)] (**8**) (Scheme 7; aebmz = 2-aminoethylbenzimidazole, ambmz = 2-aminomethylbenzimidazole),[40] as well as with two catalyst precursors similar to **4** in which the diamines were 1,2-diaminocyclohexane (chen) and 1,2-diphenylethylenediamine (dpen) instead of ethylenediamine: [$V^{IV}O$(pydx-chen)] (**9**) and [$V^{IV}O$(pydx-dpen)] (**10**).[24b] The reaction gave identical products with similar selectivity, although for the present systems the relative amounts of benzaldehyde are significantly higher than in the case of **7** and **8** (around 55% versus approximately 75% in this study) and lower than in the case of **9** and **10** (around 85% and 92%, respectively[24b]). Benzaldehyde is the product of the C–C bond cleavage of styrene, which usually forms under free-radical conditions.[50] This may be considered an indication that in the present systems the mechanism follows a similar pathway.

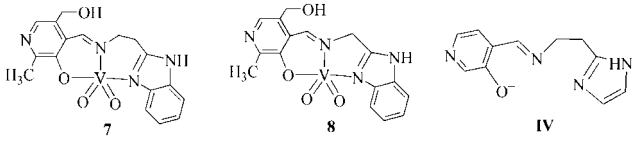

Scheme 7.

For the oxidation of hydrocarbons with transition-metal complexes as catalysts in the presence of H_2O_2, two general groups of mechanisms are usually considered: the radical and nonradical ones, both of which involve metal–peroxido intermediates. The radical mechanism is based on the formation of the free $HOO^{\cdot}$ and $HO^{\cdot}$ radicals,[51–53] the latter directly oxidizing hydrocarbons to give alkylperoxides, which then undergo decomposition to the final oxidation products. Among the nonradical pathways, the Sharpless

mechanism is usually considered to be the most favourable one for the epoxidation of olefins.[54,55]

The radical and nonradical (Sharpless-type) mechanism of epoxidation were recently studied by DFT methods for a model complex of **7** (ligand **IV**) and ethene as substrate. The radical pathway was found to be more favourable than the non-radical route. It is indeed possible that in the present systems the radical route might also be more favourable than the nonradical (Sharpless) pathway.

Conclusion

Oxidovanadium(IV)-exchanged zeolite-Y complexes [V^{IV}O(pydx-en)]-Y (**4**), [V^{IV}O(pydx-1,3-pn)]-Y (**5**) and [V^{IV}O(pydx-1,2-pn)]-Y (**6**) were synthesized and characterized by IR, UV/Vis and EPR spectroscopy, elemental analyses, thermal studies, FESEM and XRD. The corresponding neat complexes [V^{IV}O(pydx-en)] (**1**), [V^{IV}O(pydx-1,3-pn)] (**2**) and [V^{IV}O(pydx-1,2-pn)] (**3**) were also prepared.

The encapsulated complexes **4**–**6** efficiently catalyze the oxidation of styrene by H_2O_2 and with higher conversions than the corresponding neat complexes **1**–**3** or the related neat complexes [V^{IV}O(pydx-chen)] (**9**) and [V^{IV}O(pydx-dpen)] (**10**),[24b] benzaldehyde being the main product formed (around 75% under the "optimized" conditions). The encapsulated complexes **4**–**6** are also efficient catalysts for the oxidation of cyclohexene by H_2O_2, and under the "optimized" conditions, 2-cyclohexen-1-one (around 45%) and 2-cyclohexen-1-ol (around 40%) are the main products formed, followed by cyclohexane-1,2-diol. The encapsulated complexes **4**–**6** again show significantly higher conversions than the corresponding neat complexes **1**–**3** and the related neat complexes [V^{IV}O(pydx-chen)] (**9**) and [V^{IV}O(pydx-dpen)] (**10**), as well as distinct selectivity. Neat complexes **9** and **10** gave mainly cyclohexane-1,2-diol (around 70–75%), followed by 2-cyclohexen-1-ol (around 14–18%) and cyclohexane-1,2-diol (around 4–9%).[24b] The neat complexes **1**–**3** gave higher selectivity for 2-cyclohexen-1-ol and lower for 2-cyclohexen-1-one.

The encapsulated complexes **4**–**6** catalyze the oxidation by H_2O_2 of methyl phenyl sulfide efficiently. Under the conditions studied, the encapsulated complexes gave conversions of approximately 80–85%, with formation of the corresponding sulfoxide (around 75%) and sulfone (around 25%).

According to our data for the oxidation of styrene, cyclohexene and thioanisole with catalysts precursors **1**–**3** or **4**–**6**, no clear trend of different catalytic reactivity was found upon the change of the diamine of the Schiff base ligand. Additionally, for the heterogenized catalysts it appears that mass-transfer phenomena, namely, the restricted access of the oxidant and substrate to the active complex, and possibly also diffusion of products out of the zeolite, are crucial factors for the overall efficiency of the reactions. In particular, the effect of temperature is significant, probably mostly due to faster mass transfer at 80 °C than at lower temperature, and not because of thermodynamic/kinetic reasons.

The higher activity observed for the encapsulated complexes **4**–**6** and the selectivity trend of obtaining products with a higher degree of oxidation when using the encapsulated complexes, relative to the corresponding neat catalysts, may result from favourable adsorption of water and H_2O_2 to the polar surface of the zeolite cages, thus making the oxidant more easily available for reaction with the substrates.

The catalytic reactions probably proceed through the formation of [V^{V}O(O)$_2$(Schiff base)] intermediates, followed by the corresponding hydroperoxido complexes. At least in the case of styrene, by comparison with a previous mechanistic study with a distinct system[40] it is suggested that a radical pathway is preferred for the epoxidation step, this being compatible with the preferred formation of benzaldehyde.

Experimental Section

Materials and Methods: Analytical reagent-grade oxidovanadium(IV) sulfate (Loba Chemie, India), 30% aqueous H_2O_2 (Qualigens, India), pyridoxal hydrochloride (Himedia, India), methyl phenyl sulfide (Alfa Aeaser, U.S.A.), styrene (Acros Organics, U.S.A.), 1,2-diaminoethane, 1,2-diaminopropane and 1,3-diaminopropane (S.D. fine chemicals, India) were used as received. Zeolite-Y (Si/Al ≈ 10) was obtained from Indian Oil Corporation (R&D), Faridabad, India. All other chemicals and solvents used were of AR grade. Ligands H_2pydx-en (**I**), H_2pydx-1,3-pn (**II**) and H_2pydx-1,2-pn (**III**) were prepared as described in the literature.[29]

Instrumentation and Characterization Procedures: Elemental analyses of the ligands and complexes were obtained with an Elementar Vario-EL-III instrument. Vanadium was analyzed using inductively coupled plasma (ICP; Labtam 8440 plasma lab) after leaching the metal ions with very dilute aqueous KOH solution to a specific volume in a volumetric flask. Electronic spectra of encapsulated complexes were recorded in Nujol with a Shimadzu 1601 UV/Vis spectrophotometer by layering the mull of the sample inside of one of the cuvettes while keeping the other one layered with Nujol as reference. Spectra of neat complexes were recorded in methanol. IR spectra were recorded as KBr pellets with a Nicolet NEXUS Aligent 1100 series FTIR spectrometer after grinding the sample with KBr. Thermogravimetric analyses of the complexes were carried out with a Perkin–Elmer (Pyris Diamond) instrument in air with a heating rate of 10 °C min^{-1}. Scanning electron micrographs (SEMs) of encapsulated catalysts were recorded with a Leo instrument model 435VP; the samples were dusted on alumina and coated with a thin film of gold to prevent surface changing and to protect the surface material from thermal damage by the electron beam. In all analysis a uniform thickness of about 0.1 mm was maintained. Energy-dispersive X-ray analysis (EDX) was obtained with an FEI Quanta 200 FEG microscope. X-ray powder diffractograms of solid catalysts were recorded with a Bruker AXS D8 Avance X-ray powder diffractometer with a Cu-K_α target. EPR spectra were recorded with a Bruker ESP 300E X-band spectrometer. The spin Hamiltonian parameters were obtained by simulation of the spectra with the computer program of Rockenbauer and Korecz.[33] ^{51}V NMR spectra were obtained with a Bruker Avance III 400 MHz spectrometer with the common parameter settings. NMR spectra were recorded in CD_3OD, and $\delta(^{51}V)$ values are referenced relative to neat $V^{V}OCl_3$ as external standard. A thermoelectron gas chromatograph with an HP-1 capillary column (HP-1, 30 m × 0.25 mm × 0.25 μm) was used to analyze the reaction prod-

ucts. The identity of the products was confirmed by GC–MS with a Perkin–Elmer Clarus 500 instrument.

[$V^{IV}O$(pydx-en)] (1): A solution of H_2pydx-en (1.792 g, 5 mmol) in methanol (50 mL) was treated with [$V^{IV}O(acac)_2$] (1.33 g, 5 mmol) dissolved in methanol (10 mL), and the reaction mixture was heated at reflux in an oil bath for 4 h. During this period a green solid of [$V^{IV}O$(pydx-en)] slowly separated out. After cooling the mixture, it was filtered off, washed with methanol and dried. Yield 78.1%. $C_{18}H_{20}N_4O_5V$ (423.32): calcd. C 51.07, H 4.76, N 13.24; found C 49.8, H 4.8, N 13.4.

[$V^{IV}O$(pydx-1,3-pn)] (2) and [$V^{IV}O$(pydx-1,2-pn)] (3): These complexes were prepared similarly using the respective ligand.

[$V^{IV}O$(pydx-1,3-pn)] (2): Yield 88.3%. $C_{19}H_{22}N_4O_5V$ (437.35): calcd. C 52.18, H 5.07, N 12.81; found C 51.5, H 5.3, N 12.2.

[$V^{IV}O$(pydx-1,2-pn)] (3): Yield 65.4%. $C_{19}H_{22}N_4O_5V$ (437.35): calcd. C 52.18, H 5.07, N 12.81; found C 51.8, H 5.0, N 12.7.

[$V^{IV}O$]-Y [oxidovanadium(IV)-exchanged zeolite-Y]: A filtered solution of $V^{IV}OSO_4 \cdot 5H_2O$ (9 g, 36 mmol) dissolved in distilled water (100 mL) was added to a suspension of Na–Y (15 g) in distilled H_2O (800 mL), and the reaction mixture was heated at 90 °C with stirring for 24 h. The light-green solid was filtered, washed with hot distilled water until the filtrate was free from any $V^{IV}O^{2+}$ ion content and dried at 150 °C for 24 h. Yield: 14.9 g (99%). %V (ICP-MS): 4.6.

[$V^{IV}O$(pydx-en)]-Y (4): A mixture of [$V^{IV}O$]-Y (3.0 g) and H_2pydx-en (3.0 g) was mixed in methanol (40 mL) and the reaction mixture was heated at reflux for 15 h in an oil bath with stirring. The resulting material was suction filtered and dried. The crude mass was extracted with methanol using a Soxhlet extractor until the solid was free from unreacted ligand and free metal complex on the surface. After filtering, the free $V^{IV}O^{2+}$ ions present in the zeolite-Y were removed by stirring with aqueous 0.1 M NaCl solution (200 mL) for 8 h. It was finally washed with distilled water until no precipitate of AgCl was observed in the filtrate upon treatment with $AgNO_3$.

[$V^{IV}O$(pydx-1,3-pn)]-Y (5) and [$V^{IV}O$(pydx-1,2-pn)]-Y (6): Complexes [$V^{IV}O$(pydx-1,3-pn)]-Y (**5**) and [$V^{IV}O$(pydx-1,2-pn)]-Y (**6**) were prepared following a procedure similar to the one described for [$V^{IV}O$(pydx-en)]-Y (**4**).

Catalytic Activity: The catalytic potential of the compounds prepared was tested by choosing the oxidation of styrene, cyclohexene and methyl phenyl sulfide as model reactions. Thus, [$V^{IV}O$(pydx-en)]-Y (**4**), [$V^{IV}O$(pydx-1,3-pn)]-Y (**5**) and [$V^{IV}O$(pydx-1,2-pn)]-Y (**6**) were used as catalyst precursors. All catalytic reactions were carried out in a 50 mL flask fitted with a water-circulated condenser.

The progress of the reactions was monitored by gas chromatography by withdrawing small aliquots at chosen time intervals. The identity of the products was confirmed by GC–MS. For each type of reaction, the effects of various parameters, such as amounts of oxidant and catalyst as well as the temperature of the reaction mixture were studied to check their effect on the conversion and selectivity of the reaction products.

Oxidation of Styrene: In a typical reaction, styrene (0.52 g, 5 mmol) and aqueous 30% H_2O_2 (1.70 g, 15 mmol) were dissolved in acetonitrile (10 mL) and the temperature of the reaction mixture was set to 80 °C. The catalyst (0.010 g) was added to the above reaction mixture with stirring and reaction was considered to have begun. For the neat catalysts the amount used was 0.0015 g.

Oxidation of Cyclohexene: Aqueous 30% H_2O_2 (2.27 g, 20 mmol), cyclohexene (0.82 g, 10 mmol) and catalyst (0.005 g) were mixed in CH_3CN (5 mL) and the reaction mixture was heated at 80 °C with continuous stirring in an oil bath for approximately 6 h. For the neat catalysts the amount used was 0.0010 g.

Oxidation of Methyl Phenyl Sulfide: Methyl phenyl sulfide (1.24 g, 10 mmol), aqueous 30% H_2O_2 (2.27 g, 20 mmol) and catalyst (0.010 g) were dissolved in CH_3CN (5 mL) and the reaction mixture was stirred at room temperature for approximately 2.5 h. For the neat catalysts the amount used was 0.0010 g.

Acknowledgments

M. R. M. and P. S. thank the Department of Science and Technology, Government of India, New Delhi for financial support of the work. J. C. P. and A. K. thank FEDER, Fundação para a Ciência e Tecnologia, PEst-OE/QUI/UI0100/2011 and grant SFRH/BPD/34835/2007.

[1] M. R. Maurya, A. Kumar, J. Costa Pessoa, *Coord. Chem. Rev.* **2011**, *255*, 2315–2344.
[2] C. Bowers, P. K. Dutta, *J. Catal.* **1990**, *122*, 127–279.
[3] R. Raja, P. Ratnasamy, *Appl. Catal. A* **1996**, *143*, 145–158.
[4] E. Paez-Mozo, N. Gabriunas, R. Maggi, D. Acosta, P. Ruiz, B. Delmon, *J. Mol. Catal. A* **1994**, *91*, 251–258.
[5] C. R. Jacob, S. P. Varkey, P. Ratnasamy, *Appl. Catal. A* **1999**, *182*, 91–96.
[6] M. R. Maurya, S. J. J. Titinchi, S. Chand, *Appl. Catal. A* **2002**, *228*, 177–187.
[7] T. Joseph, D. Srinivas, C. S. Gopinath, S. B. Halligudi, *Catal. Lett.* **2002**, *83*, 209–214.
[8] J. Poltowicz, K. Pamin, E. Tabor, J. Haber, A. Adamski, Z. Sojka, *Appl. Catal. A* **2006**, *299*, 235–242.
[9] S. P. Verkey, C. Ratnasamy, P. Ratnasamy, *J. Mol. Catal. A* **1998**, *135*, 295–306.
[10] S. P. Verkey, C. Ratnasamy, P. Ratnasamy, *Microporous Mesoporous Mater.* **1998**, *22*, 465–474.
[11] S. P. Verkey, C. Ratnasamy, P. Ratnasamy, *Appl. Catal. A* **1999**, *182*, 91–96.
[12] S. Deshpande, D. Srinivas, P. Ratnasamy, *J. Catal.* **1999**, *188*, 261–269.
[13] D. Chatterjee, A. Mitra, *J. Mol. Catal. A* **1999**, *144*, 363–367.
[14] M. S. Niassary, F. Farzaneh, M. Ghandi, L. Turkian, *J. Mol. Catal. A* **2000**, *157*, 183–188.
[15] M. Silva, C. Freire, B. de Castro, J. L. Figueiredo, *J. Mol. Catal. A* **2006**, *258*, 327–333.
[16] T. Joseph, S. B. Halligudi, C. Satyanarayan, D. P. Sawant, S. Gopinathan, *J. Mol. Catal. A* **2001**, *168*, 87–97.
[17] M. R. Maurya, S. J. J. Titinchi, S. Chand, *Appl. Catal. A* **2002**, *228*, 177–187.
[18] M. R. Maurya, S. J. J. Titinchi, S. Chand, *J. Mol. Catal. A* **2003**, *201*, 119–130.
[19] M. R. Maurya, M. Kumar, S. J. J. Titinchi, H. S. Abbo, S. Chand, *Catal. Lett.* **2003**, *86*, 97–105.
[20] M. R. Maurya, A. K. Chandrakar, S. Chand, *J. Mol. Catal. A* **2007**, *270*, 225–235.
[21] S. Rayati, M. Koliaei, F. Ashouri, S. Mohebbi, A. Wojtczak, A. Kozakiewicz, *Appl. Catal. A* **2008**, *346*, 65–71.
[22] R. Bai, X. Fu, H. Bao, W. Ren, *Catal. Commun.* **2008**, *9*, 1588–1594.
[23] B. Gong, X. Fu, J. Chen, Y. Li, X. Zou, X. Tu, P. Ding, L. Ma, *J. Catal.* **2009**, *262*, 9–17.
[24] a) P. Adão, J. Costa Pessoa, R. T. Henriques, M. L. Kuznetsov, F. Avecilla, M. R. Maurya, U. Kumar, I. Correia, *Inorg. Chem.* **2009**, *48*, 3542–3561; b) P. Adão, M. R. Maurya, U. Kumar, F. Avecilla, R. T. Henriques, M. L. Kusnetsov, J. Costa Pessoa, I. Correia, *Pure Appl. Chem.* **2009**, *81*, 1279–1296.

[25] P. K. Saha, B. Dutta, S. Jana, R. Bera, S. Saha, K. Okamoto, S. Koner, *Polyhedron* **2007**, *26*, 563–571.
[26] M. R. Maurya, B. Singh, P. Adão, F. Avecilla, J. Costa Pessoa, *Eur. J. Inorg. Chem.* **2007**, 5720–5734.
[27] M. Salavati-Niasari, *J. Inclusion Phenom. Macrocyclic Chem.* **2009**, *65*, 349–360.
[28] M. R. Maurya, *Coord. Chem. Rev.* **2003**, *237*, 163–181.
[29] I. Correia, J. Costa Pessoa, M. T. Duarte, R. T. Henriques, M. F. M. Piedade, L. F. Veiros, T. Jackusch, A. Dornyei, T. Kiss, M. M. C. A. Castro, C. F. G. C. Geraldes, F. Avecilla, *Chem. Eur. J.* **2004**, *10*, 2301–2317.
[30] D. H. Williams, I. Fleming, *Spectroscopic Methods in Organic Chemistry,* McGraw-Hill, London, 5th ed., **1995**, pp. 18–21.
[31] L. F. Vilas Boas, J. Costa Pessoa, in: *Comprehensive Coordination Chemistry* (Eds.: G. Wilkinson, R. D. Gillard, J. A. Mc Cleverty), Oxford, Pergamon, **1987**, pp. 453–583.
[32] N. D. Chasteen, in: *Biological Magnetic Resonance* (Ed.: J. Reuben), Plenum, New York, **1981**, 53.
[33] A. Rockenbauer, L. Korecz, *Appl. Magn. Reson.* **1996**, *10*, 29–43.
[34] K. Wüthrich, *Helv. Chim. Acta* **1965**, *48*, 1012.
[35] D. Rehder, C. Weidemann, A. Duch, W. Priebsch, *Inorg. Chem.* **1988**, *27*, 584–587.
[36] N. Butenko, I. Tomaz, O. Nouri, E. Escribano, V. Moreno, S. Gama, V. Ribeiro, J. P. Telo, J. Costa Pesssoa, I. Cavaco, *J. Inorg. Biochem.* **2009**, *103*, 622–632.
[37] I. Cavaco, J. Costa Pessoa, D. Costa, M. T. L. Duarte, R. D. Gillard, P. M. Matias, *J. Chem. Soc., Dalton Trans.* **1994**, 149–157.
[38] J. Costa Pessoa, M. J. Calhorda, I. Cavaco, I. Correia, M. T. Duarte, V. Felix, R. T. Henriques, M. F. M. Piedade, I. Tomaz, *J. Chem. Soc., Dalton Trans.* **2002**, 4407–4415.
[39] G. Martini, M. F. Ottaviani, G. L. Seravalli, *J. Phys. Chem.* **1975**, *79*, 1716–1720.
[40] M. R. Maurya, M. Bisht, A. Kumar, M. L. Kuznetsov, F. Avecilla, J. Costa Pessoa, *Dalton Trans.* **2011**, *40*, 6968–6983.
[41] D. C. Crans, A. D. Keramidas, S. S. Amin, O. P. Anderson, S. M. Miller, *J. Chem. Soc., Dalton Trans.* **1997**, 2799–2812.
[42] K. Srinivasan, P. Michaud, J. K. Kochi, *J. Am. Chem. Soc.* **1986**, *108*, 2309–2320.
[43] R. Irie, Y. Ito, T. Katsuki, *Synlett* **1991**, 265–266.
[44] V. Hulea, E. Dumitriu, *Appl. Catal. A* **2004**, *277*, 99–106.
[45] S. B. Kumar, S. P. Mirajkar, G. C. G. Pais, P. Kumar, R. Kumar, *J. Catal.* **1995**, *156*, 163–166.
[46] J. D. Koola, J. K. Kochi, *J. Org. Chem.* **1987**, *52*, 4545–4553.
[47] D. Rehder, *Bioinorganic Vanadium Chemistry*, Wiley, New York, **2008**.
[48] M. A. Anderson, A. Willets, S. Allenmark, *J. Org. Chem.* **1997**, *62*, 8455–8458.
[49] H. B. ten Brink, H. E. Schoemaker, R. Wever, *Eur. J. Biochem.* **2001**, *268*, 132–138.
[50] a) A. G. J. Ligtenbarg, R. Hage, B. L. Feringa, *Coord. Chem. Rev.* **2003**, *237*, 89–101; b) A. Butler, M. J. Clague, G. E. Meister, *Chem. Rev.* **1994**, *94*, 625–638.
[51] a) G. B. Shul'pin, Y. N. Kozlov, G. V. Nizova, G. Süss-Fink, S. Stanislas, A. Kitaygorodskiy, V. S. Kulikova, *J. Chem. Soc*., *Perkin Trans. 2* **2001**, 1351–1371; b) Y. N. Kozlov, V. B. Romakh, A. Kitaygorodskiy, P. Buglyó, G. Süss-Fink, G. B. Shul'pin, *J. Phys. Chem. A* **2007**, *111*, 7736–7752.
[52] R. Z. Khaliullin, A. T. Bell, M. Head-Gordon, *J. Phys. Chem. B* **2005**, *109*, 17984–17992.
[53] M. V. Kirillova, M. L. Kuznetsov, V. B. Romakh, L. S. Shul'pina, J. J. R. Fraústo da Silva, A. J. L. Pombeiro, G. B. Shul'pin, *J. Catal.* **2009**, *267*, 140–157.
[54] D. V. Deubel, G. Frenking, P. Gisdakis, W. A. Herrmann, N. Rosch, J. Sundermeyer, *Acc. Chem. Res.* **2004**, *37*, 645–652.
[55] M. L. Kuznetsov, J. Costa Pessoa, *Dalton Trans.* **2009**, 5460–5468.

Received: June 21, 2011
Published Online: September 19, 2011

